HHS Public Access

Author manuscript

J Neurovirol. Author manuscript; available in PMC 2020 June 01.

Published in final edited form as:

J Neurovirol. 2019 June ; 25(3): 415–421. doi:10.1007/s13365-019-00740-3.

Microglial cell depletion is fatal with low level picornavirus infection of the central nervous system

John Michael S. Sanchez, BS[1], **Ana Beatriz DePaula-Silva, PhD**[1], **Daniel J. Doty, BS**[1], **Amanda Truong, BS**[2], **Jane E. Libbey, MS**[1], and **Robert S. Fujinami, PhD**[1,#]

[1]Department of Pathology, University of Utah School of Medicine, 15 North Medical Drive East, 2600 EEJMRB, Salt Lake City, UT, 84112 USA

[2]Department of Oncological Sciences, Huntsman Cancer Institute, 2000 Circle of Hope, 2724 HCI-SOUTH, Salt Lake City, UT 84112 USA

Abstract

Microglia are the only resident myeloid cell in the central nervous system (CNS) parenchyma, but the role of microglia in the context of neurotropic viral infection is poorly understood. Using different amounts of Theiler's murine encephalomyelitis virus (TMEV) in a preclinical model of epilepsy and PLX5622, a colony stimulating factor-1 receptor inhibitor that selectively depletes microglia in the CNS, we report that microglia-depleted, TMEV-infected mice develop seizures, manifest paralysis, and uniformly succumb to fatal encephalitis regardless of viral amount. CNS demyelination correlates with viral amount, however viral amount does not correlate with axon damage and TMEV antigen in the CNS.

Keywords

Microglia; Theiler's murine encephalomyelitis virus; Seizures; Paralysis; Viral encephalitis; Picornavirus

Introduction

Microglia are resident myeloid cells of the central nervous system (CNS) that are unique in their developmental origin and location in the CNS parenchyma [reviewed in (Li and Barres 2018)]. Microglia are derived primarily from yolk sac progenitors, which differentiate them from other myeloid cells that primarily originate from fetal liver progenitors and hematopoietic stem cells. Recent transcriptomic analyses have identified microglia as key players in neurodegenerative disease (Keren-Shaul et al. 2017), however the role of these CNS-resident myeloid cells in neurotropic viral infection is not as well understood.

Theiler's murine encephalomyelitis virus (TMEV) is a positive-sense, single-stranded RNA virus of the *Picornaviridae* family that is used to model epilepsy and multiple sclerosis

Correspondence to: Robert S. Fujinami, PhD, University of Utah School of Medicine, 15 North Medical Drive East, 2600 EEJMRB, Salt Lake City, UT 84112, USA, Robert.Fujinami@hsc.utah.edu, Phone: 801-585-3308, Fax: 801-585-7376.

Conflicts of Interest: The authors declare that they have no conflicts of interest.

depending on the mouse strain used [reviewed in (DePaula-Silva et al. 2017)]. Intracerebral (i.c.) TMEV infection of C57BL/6J mice leads to the development of acute seizures and, although the virus is typically cleared at 14 days post infection (p.i.), the mice go on to develop spontaneous recurrent seizures. In contrast, SJL/J mice are unable to clear TMEV infection in the CNS resulting in a chronic demyelinating disease [reviewed in (DePaula-Silva et al. 2017)].

In order to investigate the specific role of microglia in the context of TMEV CNS infection, we utilized a pharmacological inhibitor of colony stimulating factor-1 receptor (CSF-1R), PLX5622. Continuous CSF-1R stimulation is required for microglial cell survival (Elmore et al. 2014) and PLX5622 has been previously shown to specifically and substantially deplete microglia in the CNS (Dagher et al. 2015). Using PLX5622 to deplete microglia and different amounts of TMEV in C57BL/6J mice, we sought to characterize the role of microglia in neurotropic virus infection and virus-induced seizures.

We report that TMEV infection in microglial cell-depleted C57BL/6J mice uniformly results in fatal viral encephalitis, even infection with approximately 40 plaque-forming units (PFU). Seizures are still observed in microglial cell-depleted mice, but we also note subsequent development of paralysis in these mice. TMEV-infected, microglia-depleted mice exhibit demyelination, axonal damage, and TMEV antigen in the CNS. The lack of a sub-lethal amount of TMEV in the context of microglial cell depletion suggests that microglia are critical orchestrators of the antiviral response in the CNS.

Methods

Animals

C57BL/6J male mice were purchased from the Jackson Laboratory (Bar Harbor, ME). The care and use of the mice were performed in accordance with the guidelines prepared by the committee on Care and Use of Laboratory Animals, Institute of Laboratory Animals Resources, National Research Council.

PLX5622 treatment

C57BL/6J male mice (4 weeks-old) received either AIN-76A Rodent Diet without PLX5622 or AIN-76A Rodent Diet with 1,200 mg PLX5622 (Free Base)/kg (Research Diets, New Brunswick, NJ and Plexxikon, Berkeley, CA) starting 7 days prior to infection until the experimental end point. Food and water were available *ad libitum*.

Infection

C57BL/6J male mice (5 weeks-old) were anesthetized with isoflurane via inhalation and infected i.c. with 4×10^4, 4×10^3, 4×10^2, or 4×10^1 PFU (n = 5 mice per group) of the Daniels (DA) strain of TMEV. The site of injection was in the postparietal cortex of the right cerebral hemisphere to a depth of 2 mm. The needle had a William's collar to limit penetration of the tip to 2 mm. The DA strain was propagated as previously described (Tsunoda et al. 1997).

Observations

Mice were observed on Day 0 and then daily starting 3 days p.i. for weight change, seizure activity, and paralysis. Seizure activity was graded using the Racine scale as follows: stage 1, mouth and facial movements; stage 2, head nodding; stage 3, forelimb clonus; stage 4, rearing; and stage 5, rearing and falling (Benkovic et al. 2004; Racine 1972). Paralysis was scored as follows: 1, limp tail; 2, hind limb paresis; 3, abnormal gait; 4, hind limb paralysis; 5, moribund or dead (Libbey et al. 2016).

Immunohistochemistry

Mice were euthanized with isoflurane and perfused with phosphate-buffered saline (PBS), followed by a 4% paraformaldehyde phosphate-buffered solution. Brains were cut coronaly and spinal cords were cut transversely and embedded in paraffin by standard methods. Four-μm-thick tissue sections were stained with Luxol fast blue for myelin visualization. TMEV antigen and damaged axons were visualized by the avidin-biotin peroxidase complex technique, using hyperimmune rabbit serum to DA virus and SMI 311 (MilliporeSigma, Burlington, MA) to nonphosphorylated neurofilament with autoclave pretreatment, respectively (Tsunoda et al. 2003). Slides were scanned using the Pannoramic MIDI digital slide scanner, visualized using CaseViewer 2.2 digital microscope software, and quantified using QuantCenter image analysis platform (3D HISTECH Ltd., Budapest, Hungary). The amount of TMEV antigen and axon damage was calculated in brain sections by percent positive pixels divided by total non-background pixels. The extent of demyelination was calculated in annotated white matter tracts of the spinal cord by percent of light blue area divided by total tissue area.

Flow cytometry

Mice were euthanized on day 6 post mock-infection with PBS and perfused with PBS. Brain and spinal cord tissues were enzymatically dissociated with collagenase (MilliporeSigma) and DNase I (Roche, Basel, Switzerland) and subsequently mechanically dissociated by vigorous pipetting. Leukocytes were enriched by Percoll (MilliporeSigma) density gradient centrifugation. Cells were treated with Fc blocker (BioLegend, San Diego, CA), stained with the indicated anti-mouse antibodies for 30 minutes at 4°C [V500 anti-mouse CD45 (BD Bioscience, San Jose, CA), APC anti-mouse CD11b (eBioscience, San Diego, CA)], and analyzed by flow cytometry. CNS-derived cells were stained and analyzed individually for each mouse. Live cells were determined by forward and side scatter fluorescence on a BD LSRFortessa X-20 Cell Analyzer (BD Bioscience). Flow cytometry data analysis was performed using FlowJo software (FlowJo, Ashland, OR).

Results

In order to deplete microglia, C57BL/6J mice were fed *ad libitum* on chow fortified with PLX5622 (1,200 mg/kg). We first tested whether the CSF-1R inhibitor depletes microglia, as previously described (Dagher et al. 2015), by performing flow cytometry on CNS leukocytes from PBS mock-infected mice on the PLX5622-fortified diet and mice on the same diet without PLX5622. Indeed, mice on the PLX5622-fortified diet had 78.9% reduction in microglia compared to mice that did not receive PLX5622 (Fig. 1). We then

investigated the effect of microglia depletion in the context of TMEV infection by feeding mice either PLX5622-chow or control chow a week prior to i.c. TMEV infection. Infecting mice with 4×10^4 PFU of TMEV resulted in a stark disparity in survival with microglia-depleted mice uniformly succumbing to viral infection and microglia-competent mice surviving throughout the duration of observation (Fig. 2).

To assess whether there was a sub-lethal amount of TMEV in the context of microglia depletion, we infected microglia-depleted mice with either 4×10^3, 4×10^2, or 4×10^1 PFU of TMEV and monitored body weight, survival, seizures, and paralysis. Surprisingly, TMEV infection resulted in fatal encephalitis regardless of viral amount in microglia-depleted mice. By 10 days p.i., all mice had died or were moribund to the point where they needed to be sacrificed (Fig. 3). Mice infected with higher amounts of TMEV succumbed sooner than mice infected with lower amounts of TMEV. Mice infected with higher amounts of TMEV also exhibited more severe weight loss than mice infected with lower amounts of TMEV (Fig. 4). The percentage of mice with seizures was not statistically significant between different amounts of TMEV, though this may be due to the small number of animals used in the study (Fig. 5). Interestingly, we also observed the development of paralysis in these mice with similar kinetics across different amounts of TMEV (Fig. 6).

To investigate the cellular underpinnings of these observed phenotypes we performed immunohistochemistry for axonal damage, demyelination, and TMEV antigen in microglia-depleted mice infected with varying amounts of TMEV. As expected, we observed the presence of TMEV antigen in the brain parenchyma of all microglia-depleted, TMEV-infected mice (Fig. 7). Using SMI-311, which labels non-phosphorylated neurofilament as a marker of damaged axons, we detected evidence of axonal damage in the spinal cords of all microglia-depleted, TMEV-infected mice (Fig. 8). Interestingly, through Luxol fast blue staining for myelin, we observed demyelination in the spinal cords of microglia-depleted, TMEV-infected mice that correlated with the amount of TMEV used to infect the mice (Fig. 9).

Discussion

Here we demonstrate that microglial cell depletion makes mice uniquely sensitive to CNS infection with TMEV. This agrees with recent work by others investigating the role of microglia in CNS infection with TMEV (Waltl et al. 2018b) and with the JHM strain of mouse hepatitis virus (JHMV), another neurotropic virus (Wheeler et al. 2018). However, depletion of peripheral macrophages with clodronate-containing liposomes does not result in fatal encephalitis, but instead improves seizure outcomes (DePaula-Silva et al. 2018; Waltl et al. 2018a). In contrast, microglia-depleted mice maintain the development of seizures and go on to develop paralysis. Indeed, we observe histological evidence of axonal damage and demyelination, which may contribute to the development of paralysis, in microglia-depleted, TMEV-infected mice. This builds a model in which microglia and CNS-infiltrating macrophages have distinct roles in the antiviral immune response and the subsequent development of seizures and paralysis.

Among the first studies to use pharmacological depletion of microglia in the context of neurotropic viral infection, Wheeler and colleagues also observed uniform fatal viral encephalitis in the JHMV model of demyelinating disease with chronic PLX5622 treatment (Wheeler et al. 2018). They demonstrated that although immune cell infiltration into the CNS was not hampered by microglial cell depletion, the population of virus-specific $CD4^+$ T cells was significantly decreased, suggesting a suboptimal antiviral T cell response. This led to delayed viral clearance in microglial cell-depleted animals, which mirrors our observations. Interestingly, they also showed that regulatory T cells (Tregs) were significantly reduced with PLX5622 treatment and raised the possibility of an unchecked immune response contributing to host damage in their model. The fact that we see a lethal phenotype even with low amounts of TMEV suggests that the phenotype in our model is predominantly due to a fundamental inability to clear the virus as opposed to an overactive antiviral response. This is supported by similar abundance of TMEV antigen observed in microglia-depleted mice across the amounts of TMEV used to infect the mice. Thus, the role of microglia in the host antiviral response likely differs depending on the strain of neurotropic virus.

A recent study using PLX5622 in the TMEV model of epilepsy also demonstrated seizure and paralysis development as well as fatal viral encephalitis in microglial cell-depleted animals (Waltl et al. 2018b). In contrast to the JHMV model, Waltl and colleagues observe an increase in Tregs in the spinal cord and elevated interleukin (IL)-10 transcripts in the CNS of microglial cell-depleted mice. They suggest that the exaggerated anti-inflammatory response in the setting of microglial cell depletion exacerbates an inadequate antiviral response (Waltl et al. 2018b). However, microglial cell depletion in TMEV-induced demyelinating disease using SJL/J mice does not result in fatal encephalitis (data not shown). SJL/J mice have been shown to induce Tregs to a greater degree than C57BL/6J mice in response to TMEV infection, one major mechanism used to explain TMEV persistence and development of demyelinating disease of SJL/J mice (DePaula-Silva et al. 2017). Together, this suggests that Tregs may be partly to blame for the poor antiviral response with microglial cell depletion, but does not fully explain the failure to control TMEV infection in microglial cell-depleted C57BL/6J mice.

In summary, our results support the role of microglia as major orchestrators of the antiviral response in the CNS. Further research is needed to determine the particular signals that microglia provide to coordinate the antiviral response.

Acknowledgements

We would like to thank Tyler J. Hanak, PhD, for many helpful discussions. This work was supported by the National Institute of Health 5R01NS065714, 1R01NS091939 and 5T32AI055434 (J.M.S.S.).

References

Benkovic SA, O'Callaghan JP, Miller DB (2004). Sensitive indicators of injury reveal hippocampal damage in C57BL/6J mice treated with kainic acid in the absence of tonic-clonic seizures. Brain Res, 1024, 59–76. [PubMed: 15451367]

Dagher NN, Najafi AR, Kayala KM, Elmore MR, White TE, Medeiros R, West BL, Green KN (2015). Colony-stimulating factor 1 receptor inhibition prevents microglial plaque association and improves cognition in 3xTg-AD mice. J Neuroinflammation, 12, 139. [PubMed: 26232154]

DePaula-Silva AB, Hanak TJ, Libbey JE, Fujinami RS (2017). Theiler's murine encephalomyelitis virus infection of SJL/J and C57BL/6J mice: Models for multiple sclerosis and epilepsy. J Neuroimmunol, 308, 30–42. [PubMed: 28237622]

DePaula-Silva AB, Sonderegger FL, Libbey JE, Doty DJ, Fujinami RS (2018). The immune response to picornavirus infection and the effect of immune manipulation on acute seizures. J Neurovirol, 24, 464–477. [PubMed: 29687406]

Elmore MR, Najafi AR, Koike MA, Dagher NN, Spangenberg EE, Rice RA, Kitazawa M, Matusow B, Nguyen H, West BL, Green KN (2014). Colony-stimulating factor 1 receptor signaling is necessary for microglia viability, unmasking a microglia progenitor cell in the adult brain. Neuron, 82, 380–397. [PubMed: 24742461]

Keren-Shaul H, Spinrad A, Weiner A, Matcovitch-Natan O, Dvir-Szternfeld R, Ulland TK, David E, Baruch K, Lara-Astaiso D, Toth B, Itzkovitz S, Colonna M, Schwartz M, Amit I (2017). A Unique Microglia Type Associated with Restricting Development of Alzheimer's Disease. Cell, 169, 1276–1290.e17 [PubMed: 28602351]

Li Q, Barres BA (2018). Microglia and macrophages in brain homeostasis and disease. Nat Rev Immunol, 18, 225–242. [PubMed: 29151590]

Libbey JE, Doty DJ, Sim JT, Cusick MF, Round JL, Fujinami RS (2016). The effects of diet on the severity of central nervous system disease: One part of lab-to-lab variability. Nutrition, 32, 877–883. [PubMed: 27133811]

Racine RJ (1972). Modification of seizure activity by electrical stimulation. II. Motor seizure. Electroencephalogr Clin Neurophysiol, 32, 281–294. [PubMed: 4110397]

Tsunoda I, Kuang LQ, Libbey JE, Fujinami RS (2003). Axonal injury heralds virus-induced demyelination. Am J Pathol, 162, 1259–1269. [PubMed: 12651618]

Tsunoda I, McCright IJ, Kuang LQ, Zurbriggen A, Fujinami RS (1997). Hydrocephalus in mice infected with a Theiler's murine encephalomyelitis virus variant. J Neuropathol Exp Neurol, 56, 1302–1313. [PubMed: 9413279]

Waltl I, Kaufer C, Broer S, Chhatbar C, Ghita L, Gerhauser I, Anjum M, Kalinke U, Loscher W (2018a). Macrophage depletion by liposome-encapsulated clodronate suppresses seizures but not hippocampal damage after acute viral encephalitis. Neurobiol Dis, 110, 192–205. [PubMed: 29208406]

Waltl I, Kaufer C, Gerhauser I, Chhatbar C, Ghita L, Kalinke U, Loscher W (2018b). Microglia have a protective role in viral encephalitis-induced seizure development and hippocampal damage. Brain Behav Immun.doi: 10.1016/j.bbi.2018.09.006.

Wheeler DL, Sariol A, Meyerholz DK, Perlman S (2018). Microglia are required for protection against lethal coronavirus encephalitis in mice. J Clin Invest, 128, 931–943. [PubMed: 29376888]

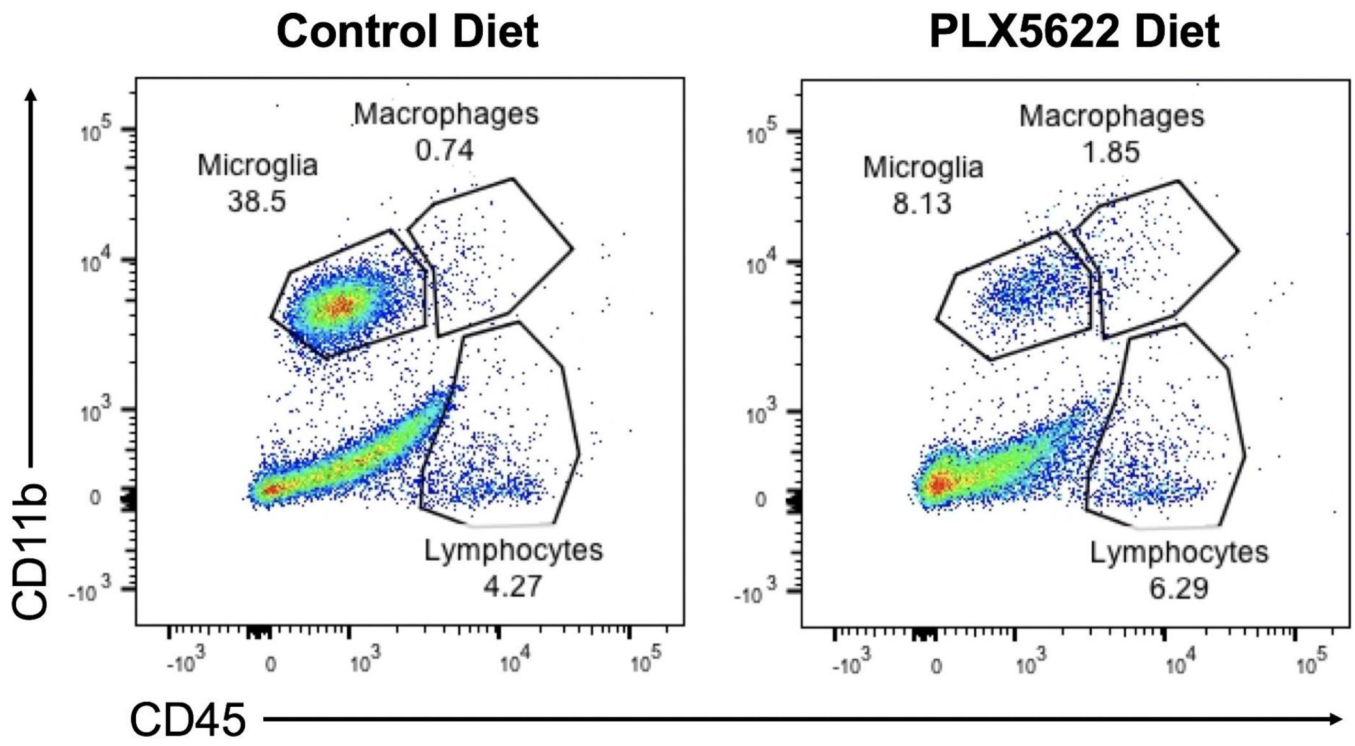

Fig 1.

PLX5622 depletes microglia in the CNS. Mice were fed with either PLX5622-fortified diet or control diet for a week prior to mock infection with PBS. Single cell suspensions were obtained from combined brain and spinal cord samples and analyzed via flow cytometry.

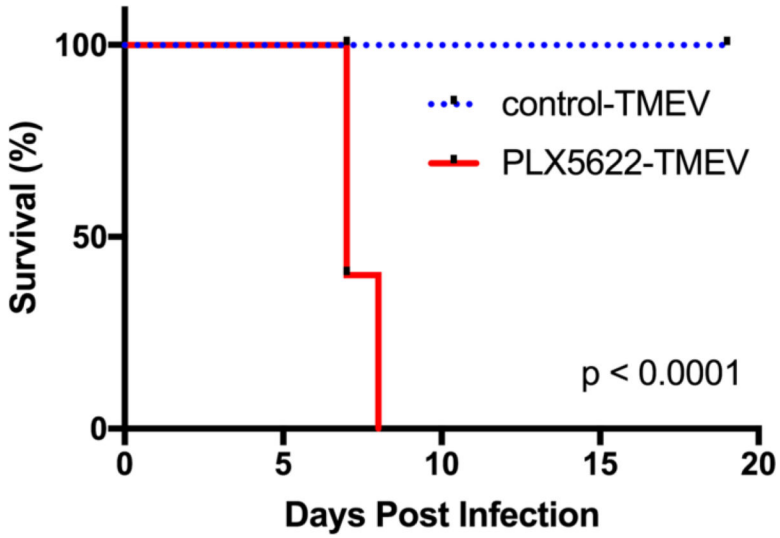

Fig 2.

Microglia depletion results in fatal encephalitis. Microglia-depleted mice and microglia-competent mice infected with 4×10^4, plaque forming units (PFU) of Theiler's murine encephalomyelitis virus (TMEV) were observed for 19 days post infection (p.i.). Mortality represented as percent daily survival of animals in comparison to day 0 (n = 10 mice per group at the start of the experiment; $p < 0.0001$; log-rank test).

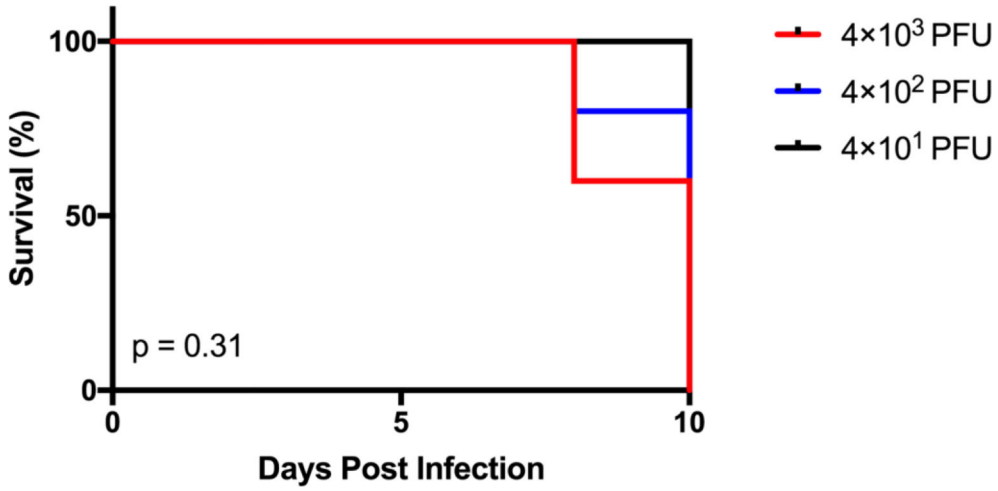

Fig 3.

There is no sub-lethal amount of TMEV in the context of microglia depletion. Microglia-depleted mice infected with 4×10^3, 4×10^2, or 4×10^1 plaque forming units (PFU) of Theiler's murine encephalomyelitis virus (TMEV) were observed for 10 days post infection (p.i.). Mortality represented as percent daily survival of animals in comparison to day 0 (n = 5 mice per group at the start of the experiment).

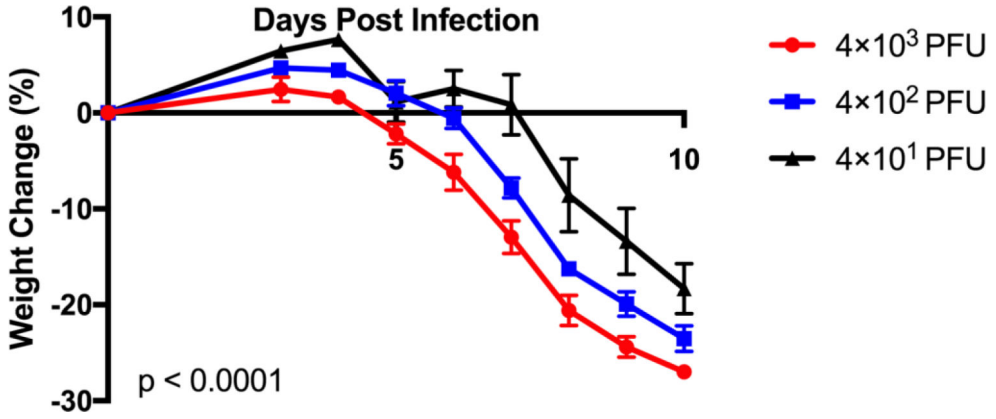

Fig 4.

Weight loss correlates with the amount of TMEV used to infect the mice. Microglia-depleted mice infected with 4×10^3, 4×10^2, or 4×10^1 PFU of TMEV were weighed daily from days 3 to 10 p.i. Weight change represented as percent daily weight in comparison to weight at day 0, given as mean ± standard error of the mean (SEM) (n = 5 mice per group at the start of the experiment; $p < 0.0001$; two-way analysis of variance/ANOVA).

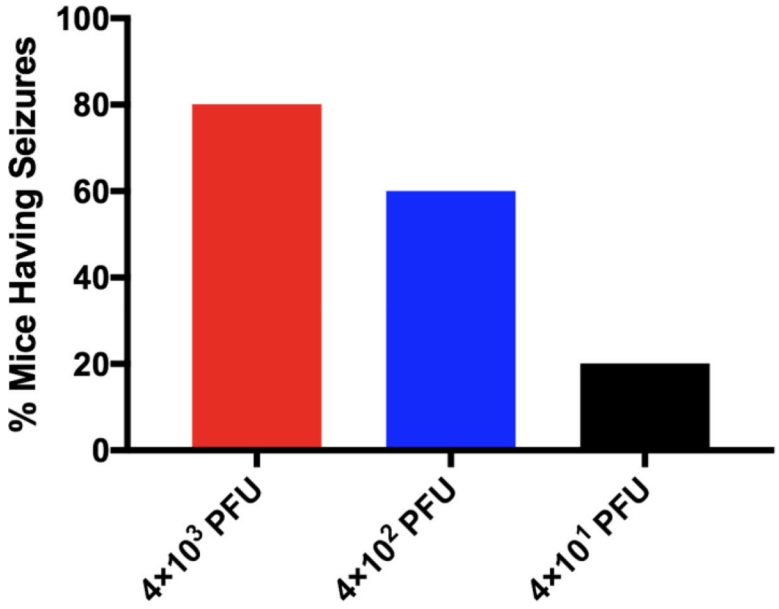

Fig 5.

Microglia-depleted mice are not protected from TMEV-induced seizures. Microglia-depleted mice infected with 4×10^3, 4×10^2, or 4×10^1 PFU of TMEV were observed daily from days 3 to 10 p.i. Percent of mice having seizures (Racine scale, stages 3 to 5) was calculated as follows: (number of mice with seizures/total number of mice infected) × 100. Percent of mice having seizures given as the mean (n = 5 mice per group at the start of the experiment; $p > 0.05$; Chi-squared test).

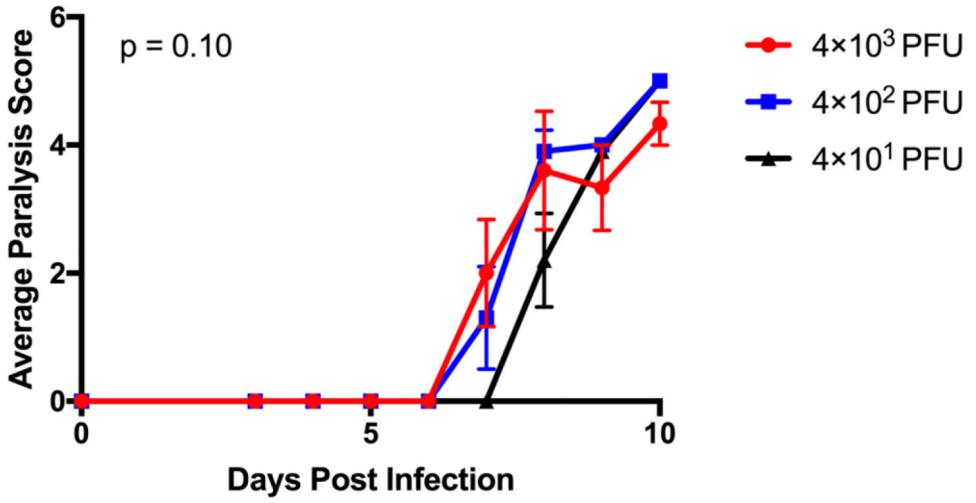

Fig 6.

Paralysis manifests in microglia-depleted mice infected with TMEV. Microglia-depleted mice infected with 4×10^3, 4×10^2, or 4×10^1 PFU of TMEV were observed daily from days 3 to 10 p.i. Average paralysis score given as the mean ± SEM (n = 5 mice per group at the start of the experiment; p = 0.10; two-way ANOVA).

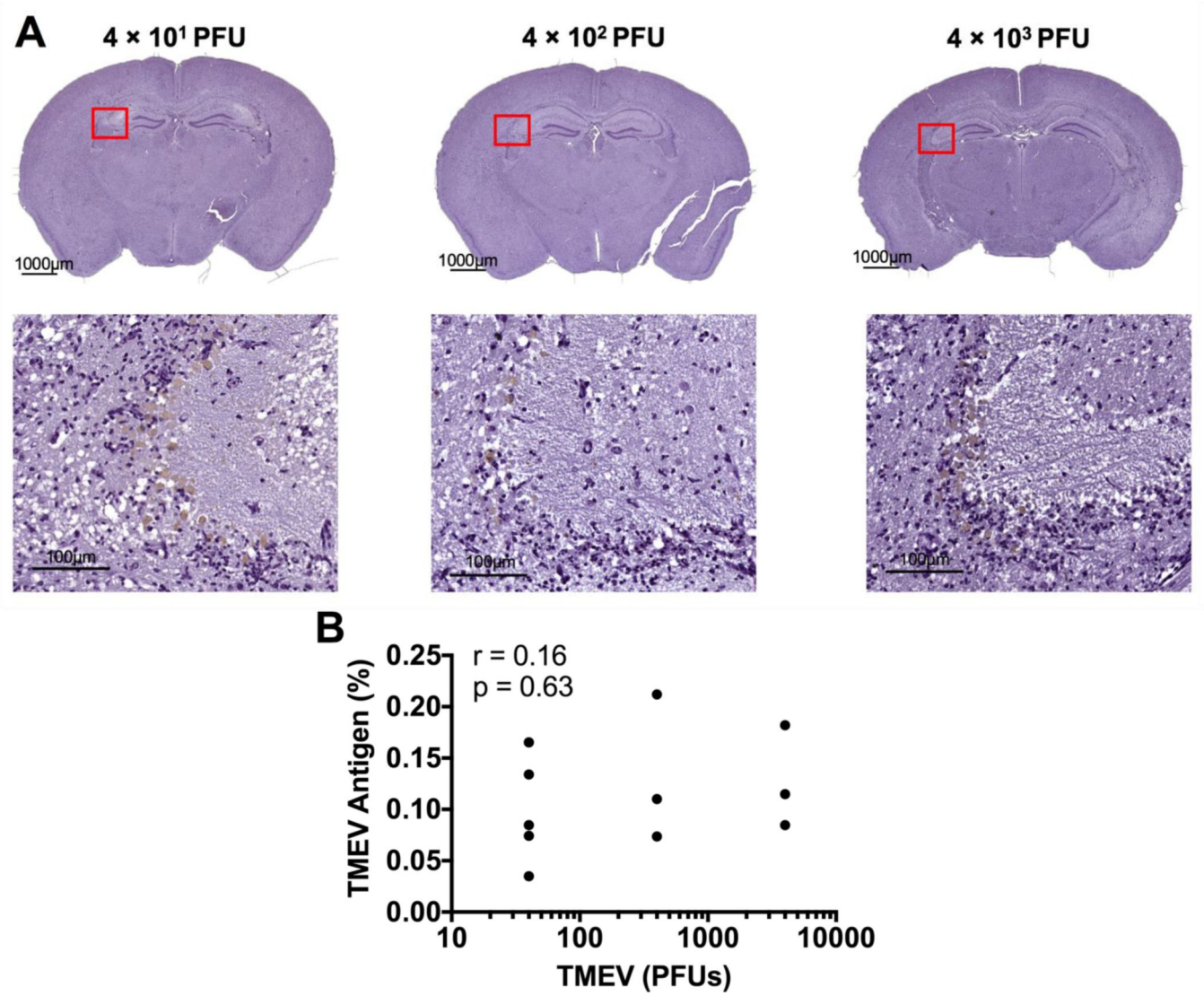

Fig 7.

TMEV antigen load in the brain does not correlate with the amount of TMEV used to infect the mice. Hyperimmune rabbit sera to TMEV was used to stain TMEV antigen in the brains of microglia-depleted mice. (A) Representative images of brain TMEV antigen load with varying TMEV amount, as indicated. (B) Pearson correlation analysis does not show significant correlation between quantified TMEV antigen staining and the amount of TMEV used to infect the mice. (n = at least 3 mice per group and at least two sections per mouse; r = 0.16; p = 0.63).

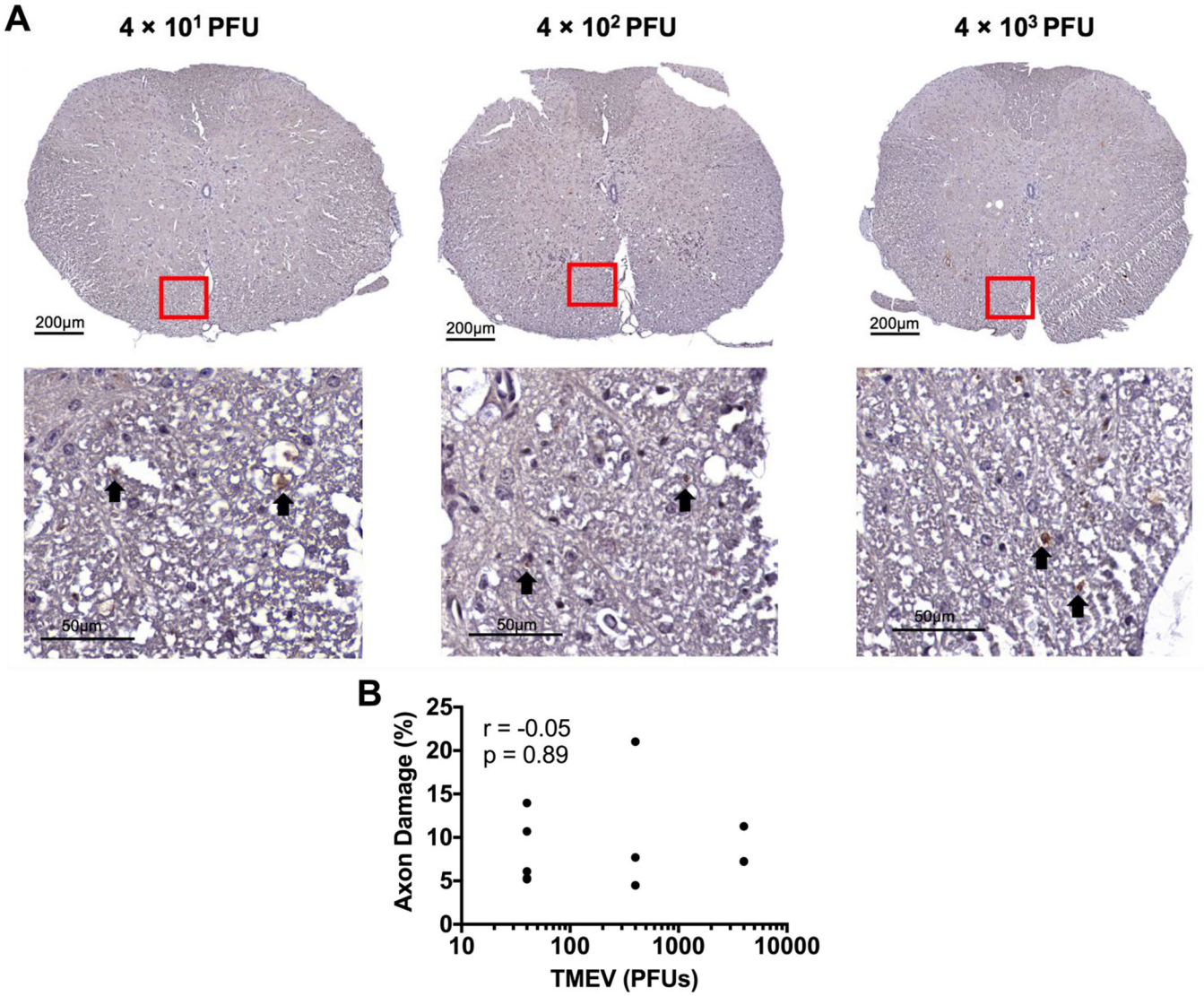

Fig 8.

The extent of spinal cord axonopathy does not correlate with the amount of TMEV used to infect the mice. We visualized damaged axons using SMI-311, which labels non-phosphorylated neurofilament. (A) Representative images of spinal cord axonopathy (arrows point to SMI-311^{+} axons) with varying TMEV amount, as indicated. (B) Pearson correlation analysis does not show significant correlation between quantified SMI-311 staining and the amount of TMEV used to infect the mice. (n = at least 3 mice per group and at least two sections per mouse; r = −0.05; p = 0.89).

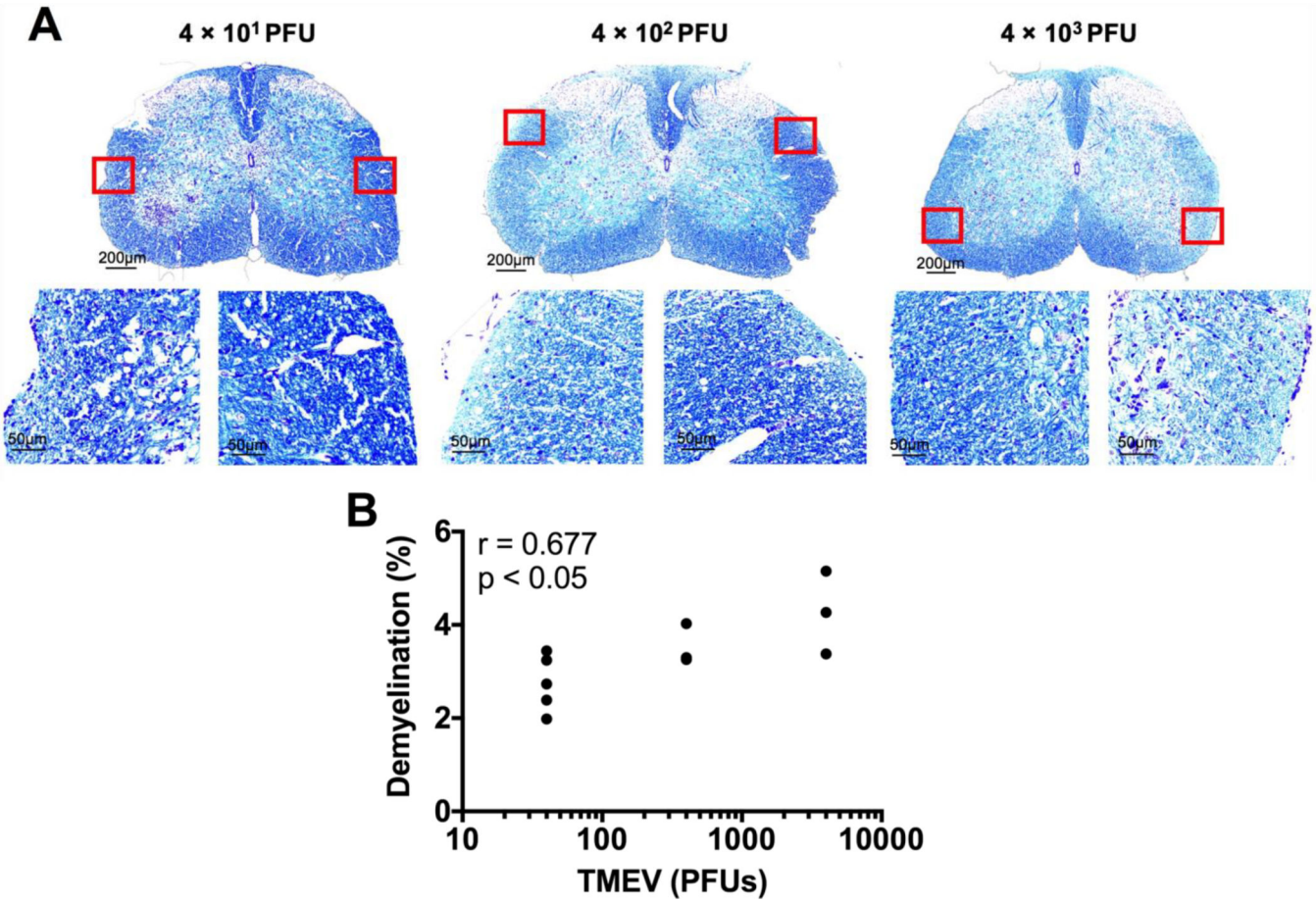

Fig 9.

Spinal cord demyelination increases with the amount of TMEV used to infect the mice. Luxol fast blue was used to stain for myelin. (A) Representative images of spinal cord demyelination with varying TMEV amount, as indicated. (B) Pearson correlation analysis shows significant correlation between quantified demyelination and the amount of TMEV used to infect the mice. (n = at least 3 mice per group and at least two sections per mouse; r = 0.667; $p < 0.05$).